Off-axis scatter measurement of the Mars Reconnaissance Orbiter (MRO) Optical Navigation Camera (ONC)

John L. Stauder*[a], Andrew E. Lowman[b], Dave Thiessen[b], Darryl Day[b], D.O. Miles[a]
[a]Space Dynamics Laboratory, Utah State University, Logan, UT 84321;
[b]Jet Propulsion Laboratory, California Institute of Technology, Pasadena, CA 91109

ABSTRACT

The Optical Navigation Camera (ONC) is part of NASA's Mars Reconnaissance Orbiter (MRO) scheduled for an August 2005 launch. The design is a 500 mm focal length, F/8.3 Ritchey-Chrétien with a refractive field corrector. Prior to flight, the off-axis performance of the ONC was measured at visible wavelengths in the off-axis scatter facility at the Space Dynamics Laboratory (SDL). This unique facility is designed to minimize scatter from the test setup to prevent data corruption. Testing was conducted in a clean room environment, and the results indicate that no detectable contamination of the optics occurred during testing. Measurements were taken in two time frames to correct an unanticipated stray light path, which occurred just outside of the sensor's field-of-view. The source of the offending path was identified as scatter from the edges of the field corrector lenses. Specifically, scatter from the interface between the flat ground glass and polished surfaces resulted in significant "humps" in the off-axis response centered at ± 1.5°. Retesting showed the removal of the humps, and an overall satisfactory performance of the ONC. The troubleshooting, correction, and lessons learned regarding the above stray light path was reported on in an earlier paper. This paper discusses the measurement process, results, and a comparison to a software prediction and other planetary sensors. The measurement validated the final stray light design and complemented the software analysis.

Keywords: off-axis scatter, stray light, PSRR, NDI, MRO, ONC, ASAP

1. INTRODUCTION

NASA's Mars Reconnaissance Orbiter (MRO) will study the water history of the red planet from orbit[1]. It is scheduled to launch in August 2005, and will arrive at Mars seven months later. The spacecraft will include the experimental navigation instrument, Optical Navigation Camera (ONC), whose objective is to provide increased placement accuracy of future landers. Prior to orbit insertion, the ONC will acquire images of Mars' moons Phobos and Deimos with stars in the background. These images will allow for improved positional accuracy of the spacecraft relative to the planet. The ONC optical layout is shown in Figure 1. It is a Ritchey-Chrétien design with a refractive field corrector. The aperture size of 6 cm and effective focal length of 50 cm make it an F/8.3 system. Since Mars will be as close as 0.4° from the edge of the sensor's field-of-view (FOV), stray light rejection is critical to mission success. A stray light analysis was included as part of the optical design process[2]. Subsequent improvements to the design were made and the final analysis showed that the ONC would marginally meet stray light requirements. Since software analysis is dependent on surface scatter estimates and programmer expertise, JPL decided to have a stray light measurement made to verify the computer analysis. The description and results of the measurement are the subject of this paper.

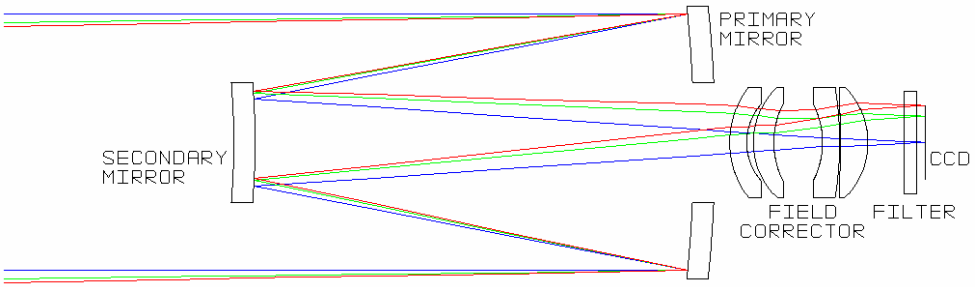

Figure 1. ONC optical layout.

*Contact: John.Stauder@sdl.usu.edu; phone 1 435-797-4388; www.sdl.usu.edu

Current Developments in Lens Design and Optical Engineering VI,
edited by Pantazis Zakos Mouroulis, Warren J. Smith, R. Barry Johnson,
Proceedings of SPIE Vol. 5874 (SPIE, Bellingham, WA, 2005) · 0277-786X/05/$15

2. OFF-AXIS SCATTER FACILITY

The off-axis scatter facility at SDL has been used to test several spaceborne sensors[3-5], including the Galileo Solid State Imaging (SSI) camera, Cassini Narrow Angle Camera (NAC), and the TIMED SABER instrument. Entrance to the room requires the passage through an air shower, which removes loose particles from the occupant. The walls, ceiling, and other components of the room are coated with a diffuse black paint to absorb and scatter incident light. The floor is covered with black carpet, whose fibers are resistant to detachment. The measurement setup located inside the room is depicted in Figure 2. Major components include the specular chamber, HEPA filters (not shown), visible source with collimator, light trap, rotary table, and photomultiplier tube (PMT). The instrument under test (IUT) is mounted on the centrally located rotary table. The HEPA filter assembly is placed above the chamber to establish a clean room environment. The filtered air is forced into the chamber from above and exits at floor level beneath the raised chamber walls. Once outside the chamber it returns to the filters, creating a circular airflow. Inside the chamber, a class 100 clean room environment is maintained. A certified particle counter is used to monitor particulates near the aperture of the IUT prior to measurements. Typically, less than 5 particles having a diameter of 0.5 μm or less register in 1 minute.

The collimated light, which represents radiation from a distant source, enters the chamber through a 10-inch hole and completely fills the entrance aperture of the IUT. The off-axis response is obtained by incrementally rotating the IUT and recording the power on the focal plane. Light that does not intersect the instrument exits the chamber where it is trapped. The chamber's specular black walls redirect light that is scattered off the IUT so that it does not directly re-enter the telescope aperture (see Figure 2 ray trace). A ray loses energy each time it encounters a wall surface. After several reflections, the light rays are reduced to negligible levels.

The rotary table, source, and PMT are controlled from outside of the room via appropriate wires and cables. The visible source is a forced-air-cooled tungsten halogen lamp with variable intensity. A small aperture is placed in front of the enclosed lamp, at the focus of the collimating optics. A baffle tube extends from the lamp to define the cone of light emanating from the pinhole. The intensity and diameter of the collimated beam can be adjusted by changing the size of the pinhole and baffle opening, respectively. The high precision rotary table is motioned by a stepping motor controller connected to a personal computer (PC). Visible light is collected by a PMT module, which is commanded and readout via a serial cable connected to the PC. The spectral range of the PMT is 0.3 to 0.65 μm, with peak sensitivity at 0.4 μm.

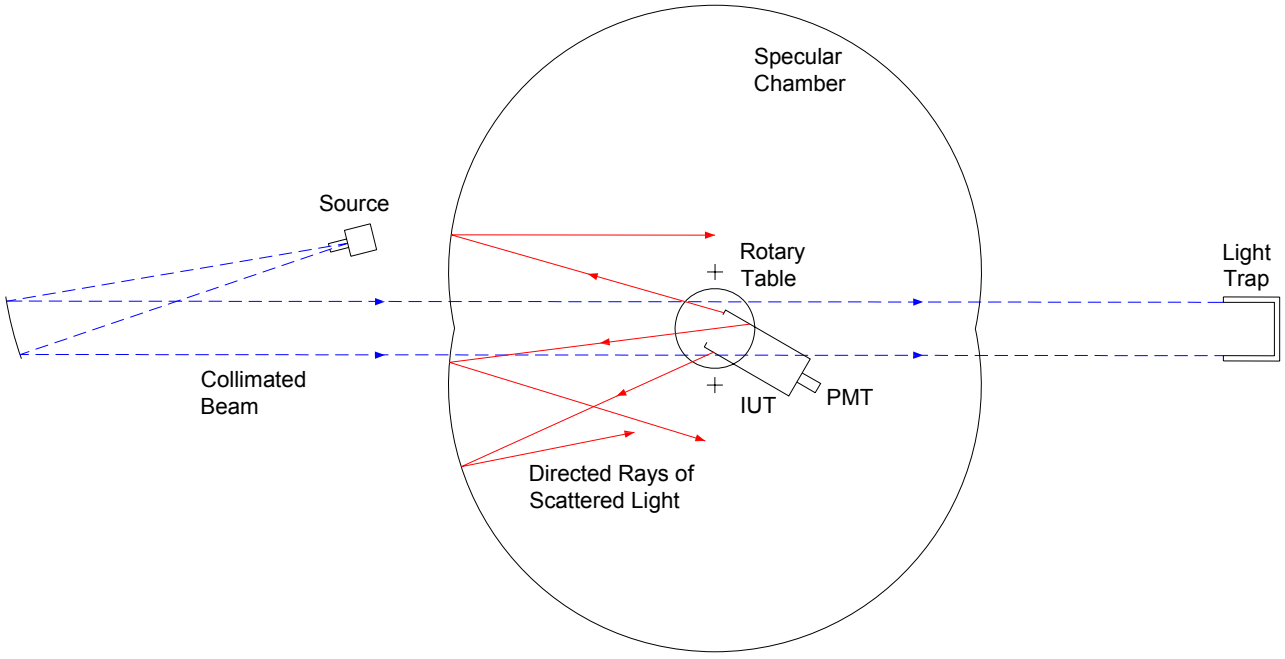

Figure 2. Measurement setup of the off-axis scatter facility.

3. OFF-AXIS MEASUREMENT PREPARATION

Preparation for the ONC measurement consisted of five tasks. They are: 1) test plan write-up, 2) facility cleanup and organization, 3) setup and verification of the testing components, 4) initiation of clean room environment, and 5) system integration and verification. This section describes aspects of the source and operational checkout of the system.

3.1 Beam uniformity measurement

The uniformity of the collimating beam was measured by taking incremental readings across the beam in the horizontal direction. The initial results showed significant non-uniformity near one edge of the 10.5 cm beam due to spatial separations in the bulb's filaments. The bulb's position behind the pinhole was adjusted to get acceptable results. The beam uniformity shown in Figure 3 is 90% across a 6.25 cm span. A vertical scan was not made.

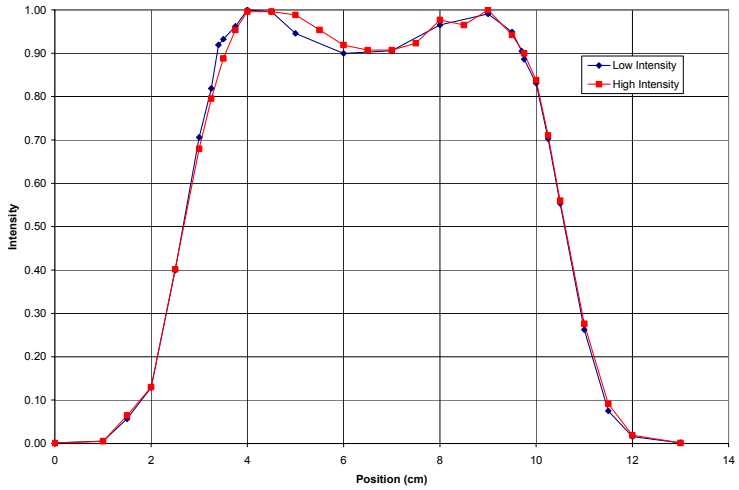

Figure 3. Collimated beam uniformity.

3.2 Source scatter angle

The off-axis angle where scattered light from the collimating mirror begins to contribute to the response is called the source scatter angle. It is dependent on the sensor aperture size, beam size, and the distance that separates the sensor and mirror. Referring to Figure 4, the angle is given by

$$\theta = \tan^{-1} \frac{R_{beam} + R_{aper}}{D} \tag{1}$$

and is measured from the edge of the field-of-view (FOV).

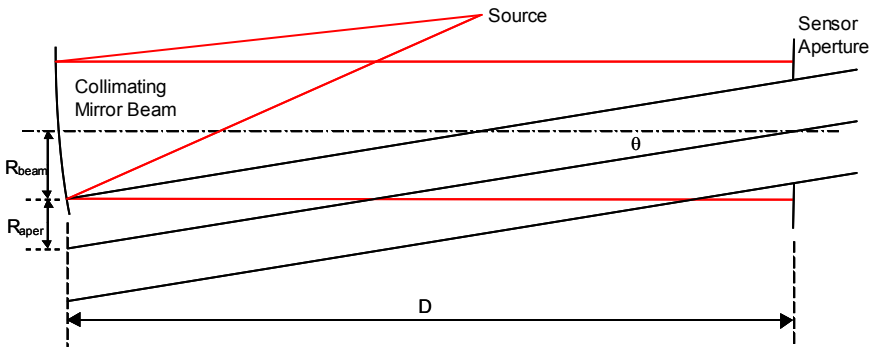

Figure 4. Source scatter angle of the collimating mirror.

To achieve the desired scatter angle of less than 1°, the mirror and sensor were separated a distance of 514.4 cm. The radii of the ONC aperture and the collimated beam are 3.0 cm and 5.25 cm, respectively. These values give a source scatter angle of 0.92° for the ONC measurement.

3.3 Operational checkout

An operational checkout of the facility was performed prior to the arrival of the ONC using a lens/baffle setup as the IUT. The simple system is shown in Figure 5 and has a 2.5° half-angle FOV. The test baffle off-axis response is shown in Figure 6. The exercise provided a system level check and determined the readiness of the facility for the ONC measurement.

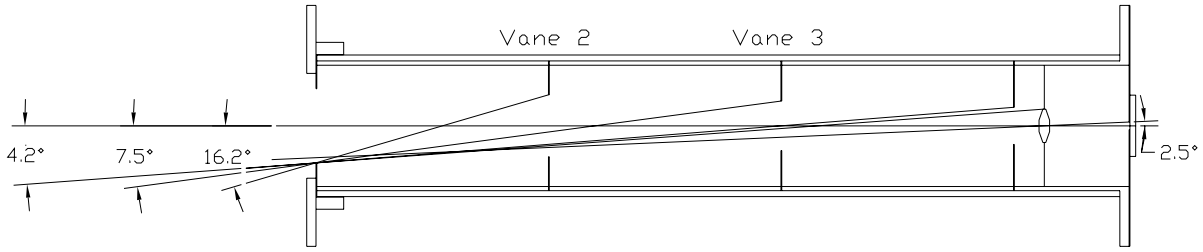

Figure 5. Test baffle configuration.

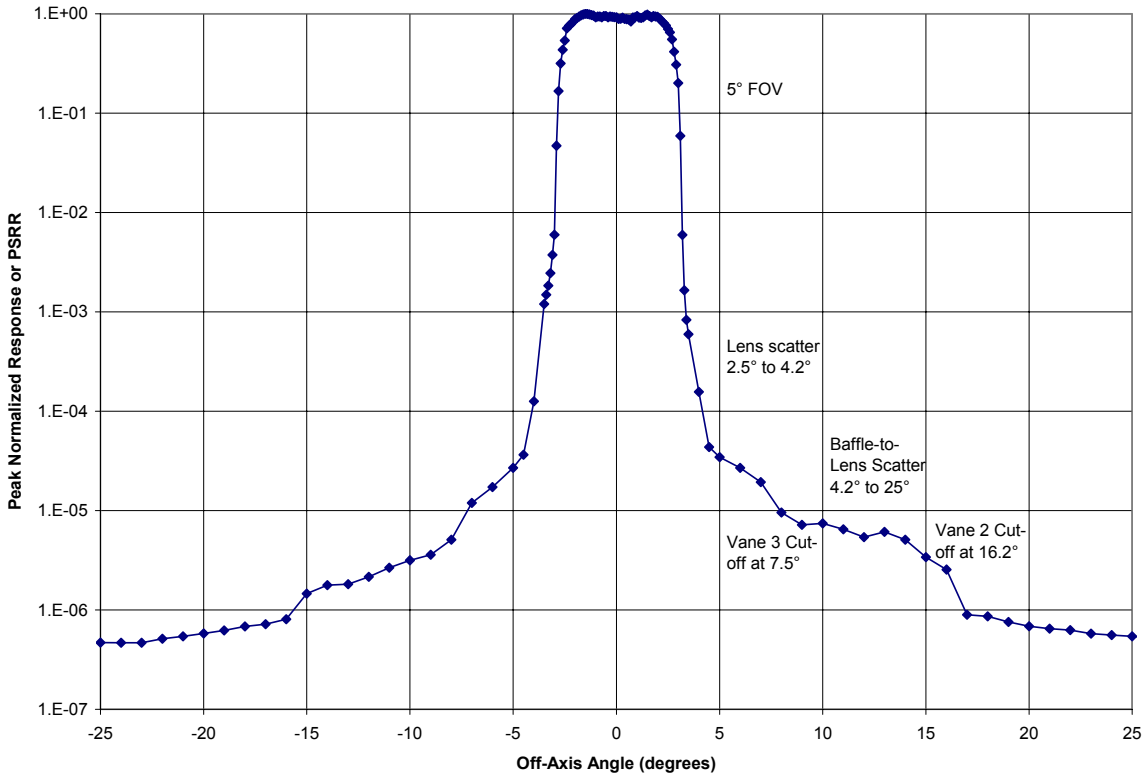

Figure 6. Measured off-axis response of the test baffle.

4. OFF-AXIS MEASUREMENT OF THE ONC

The ONC flight and engineering model (EM) cameras arrived at SDL on November 11, 2003 in an environmentally sealed container. The flight ONC was removed from the container within the specular chamber, and was mounted to the rotary table using a JPL provided fixture. A certified particle counter was used to monitor the contamination level inside of the chamber. Although the room is not a certified clean room, it consistently measured better than Class 100 operationally within the chamber.

The original plan called for testing both the flight and engineering model (EM) cameras; however, the planned EM tests were used to re-test a modified flight unit in February 2004. Correction of the flight camera was necessitated by the discovery of a critical stray light path during the initial flight camera tests. Twelve measurements were made, covering an off-axis source angle range of -70° to 70°. Measurements 1 through 5 were made on the original flight unit, and the corrected camera was tested during measurements 6 through 12. Table 1 lists the measurements performed, along with the tested configuration. The original flight unit is referred to as ONC 1, whereas the modified flight camera is identified as ONC 2. The source elevation angles were obtained by commanding the rotary table through a series of angles. The rotational position of the ONC in the mounting fixture (about the optical axis) determined the azimuthal angle. The main effect of the rotation is to change the secondary support spider with respect to the off-axis source plane. Figure 7 shows the spider orientation for rotations of 0°, 45°, and 90°.

Table 1. ONC measurement configurations.

Meas.	Camera	Elevation Ang.	Azimuth Ang.	Detector FOV	Detector Position
1	ONC 1	-25° to +25°	0°	0.14°	Center
2	ONC 1	-60° to +60°	0°	0.14°	Center
3	ONC 1	-50° to +50°	0°	0.14°	Right Edge
4	ONC 1	-50° to +50°	0°	0.14°	Left Edge
5	ONC 1	-50° to +60°	0°	1.5° x 1.5°	Center
6	ONC 2	-60° to +60°	0°	0.14°	Center
7	ONC 2	-60° to +70°	0°	0.14°	Center
8	ONC 2	-70° to +70°	0°	0.14°	Left Edge
9	ONC 2	-60° to +60°	90°	0.14°	Center
10	ONC 2	-60° to +60°	90°	0.14°	Center
11	ONC 2	-70° to +60°	90°	1.5° x 1.5°	Center
12	ONC 2	-60° to +60°	45°	0.14°	Center

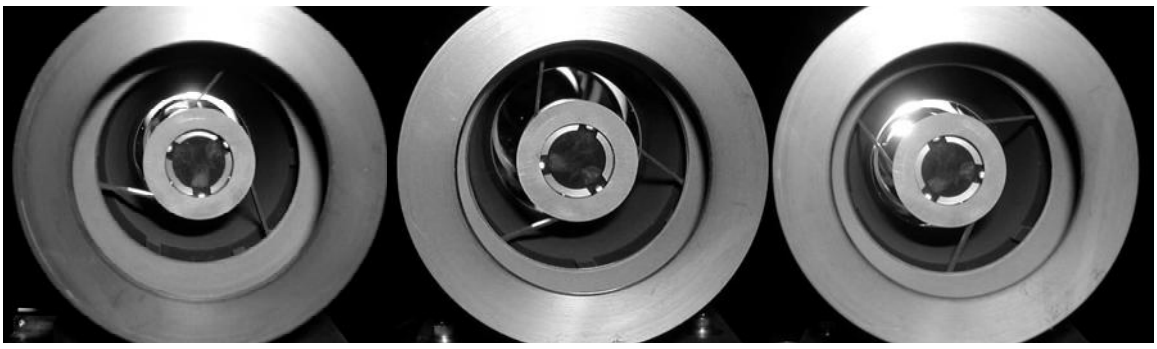

(a) (b) (c)

Figure 7. Secondary spider orientation for rotations of (a) 0°, (b) 45°, and (c) 90°.

Small and full-field measurements were made. A 0.45-0.65 μm passband filter with a square mask was located near the image plane. For most of the tests, a 1.2 mm circular aperture was placed either at the center or the edge of the mask to define a full-angle FOV of 0.14°. With the small aperture removed, the 1.33x1.33 cm mask defines a full-field of approximately 1.5°x1.5°, which is slightly larger than the design FOV of 1.4°x1.4°.

The collimated source was aligned to the ONC by adjusting the rotary table so that the source pinhole was imaged in the center of the 1.2 mm aperture. Small vertical adjustments were made using the JPL mounting fixture. During the February tests, an improved fixture was used, which made the vertical alignment easier. Once aligned, the PMT was mated to the camera and measurements were ready to be made (Figure 8).

The results of the measurements are generally presented in peak-normalized form, often called the point source rejection ratio (PSRR). The PSRR is related to the normalized detector irradiance (NDI) by the ratio of the entrance pupil and detector areas, multiplied by the system transmission τ. That is

$$NDI(\theta) = \tau \times \frac{A_{EntrPupil}}{A_{Det}} \times PSRR(\theta) \tag{2}$$

The derivation of this relation is given in the ONC stray light measurement report[6] and is available upon request. Note that the predicted transmission of the ONC is 70%.

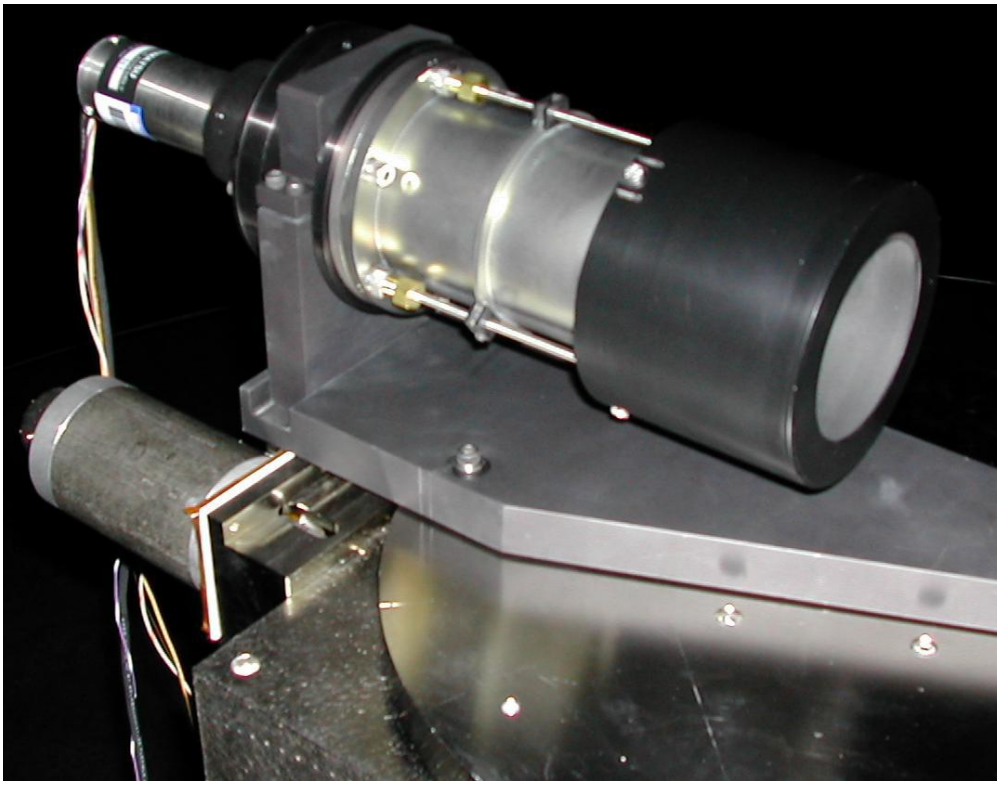

Figure 8. ONC with PMT on rotary table (improved mount shown).

4.1 Measurements 1 through 5

The ONC was in the non-rotated (Az = 0°) position on the rotary table for the first five measurements. The 1.2 mm aperture was located in the center of the image plane for Measurements 1 and 2. The initial readings indicated very poor performance, so testing was stopped to check the alignment. The PMT was removed and a visual inspection through the 1.2 mm aperture showed that the vertical alignment was off. It was corrected by adjusting the torque on the ONC mounting flange and testing resumed.

Measurements 1 and 2 are shown in Figure 9 for the full source angular range (left) and at small angles (right). The charts demonstrate excellent repeatability. The data were taken on different days indicating a stable environment and no contamination of the optics. The undesirable "humps" centered at ±1.5° are significant stray light performance degradations. Recall that Mars will be as close as 0.4° from the edge of the FOV, or 1.1° from the center of the field.

The 1.2 mm aperture was placed at the right and left edges of the focal plane (as viewed from behind the ONC) for Measurements 3 and 4, respectively. The PSRRs shown in Figure 10 indicate an asymmetric response. The responses somewhat mirror each other about the 0° position. A spike is observed at the +1.2° and –1.2° for PSRRs 3 and 4, respectively.

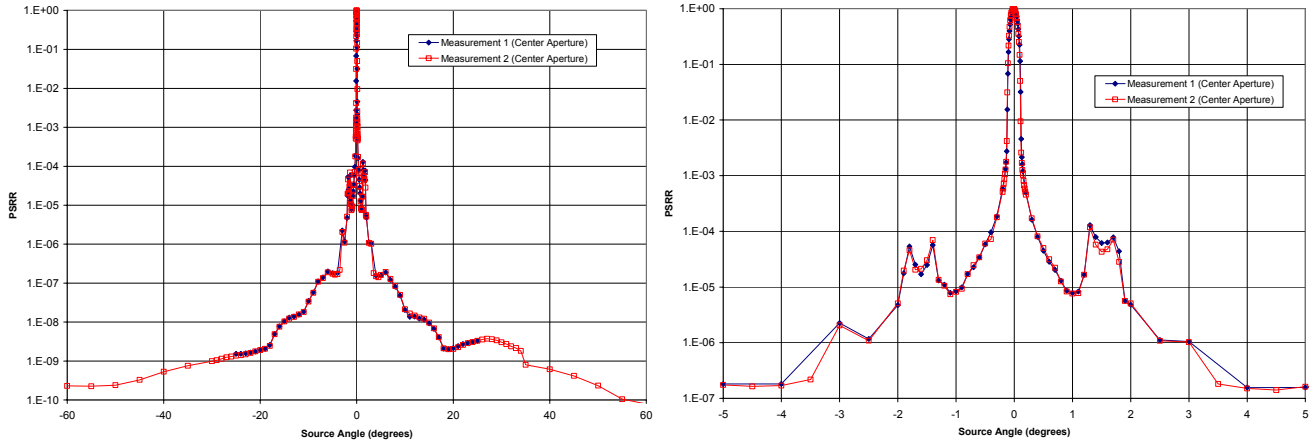

Figure 9. Measurements 1 and 2 (center aperture): PSRR at all source angles (left) and at small angles (right).

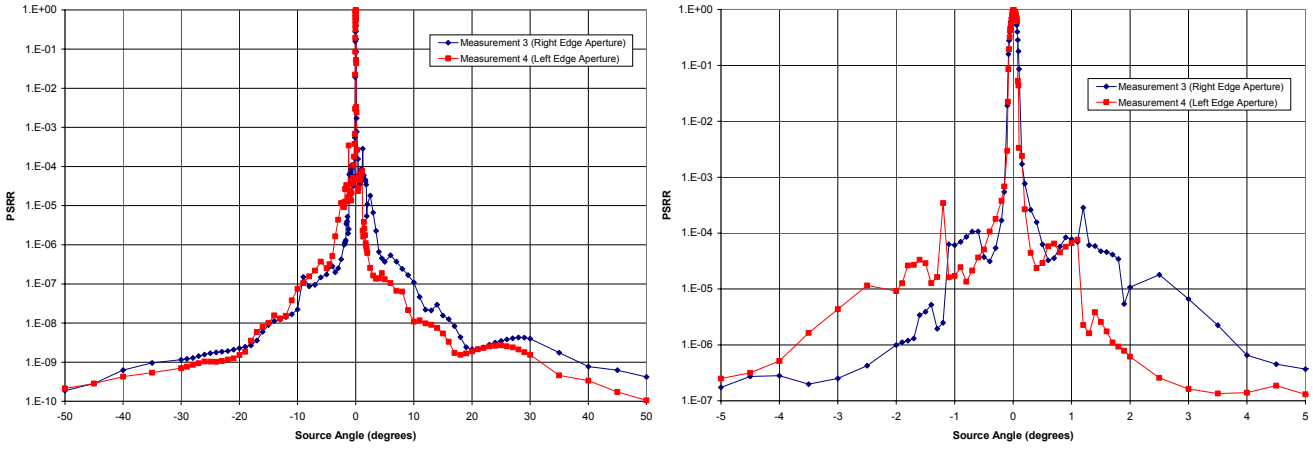

Figure 10. Measurements 3 and 4: Edge apertures.

Measurement 5 represents the full-field configuration of the ONC. The 1.2 mm aperture was removed from the image plane and the rectangular mount of the filter defined the field stop in front of the PMT. The results of this test are shown in Figure 11. Since the PSRR is a function of detector size, a direct comparison with the small-field data requires a conversion to another form of the point source transmission curve. The NDI is chosen, and the small-field and full-field results are compared in Figure 12. Note that only the off-axis portions of the curves are comparable.

The decision was made by JPL to stop testing after Measurement 5 to correct the stray light path near source angles of ±1.5°. The ONC units were taken back to JPL for analysis, and four modifications were made to the flight unit. First, three socket head screws used in the secondary mount structure were replaced with low profile ones. The original screws were viewable from the focal plane. Second, an annulus was attached to the back of the secondary conical baffle to cover a seam, which allowed light to leak around the secondary mirror. This too was visible from the detector; however, at cold temperatures the mechanical gap was expected to close. The ONC was tested warm. The third change slightly reduced the size of aperture stop, located at the primary mirror, to the design specification of 6 cm. The final fix was to mask down the aperture of two of the lenses with black paint. Using collimated light to illuminate the ONC and placing a digital camera near the focal plane, JPL personnel witnessed noticeably less scattered light. It is thought that scatter from the interface between the lens flat ground glass and polished surfaces resulted in the offending "humps". In addition to these modifications, the optics were cleaned to remove particulate contamination witnessed during the November tests. The reader is referred to a prior paper[7], which describes the troubleshooting process and stray light lessons learned for the ONC.

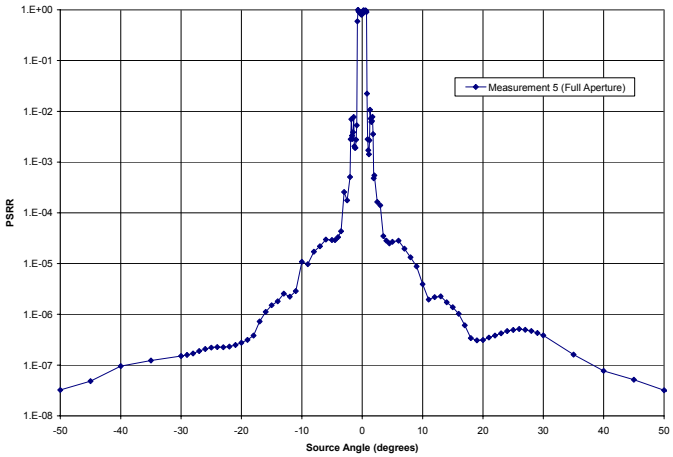

Figure 11. Measurement 5: Full aperture.

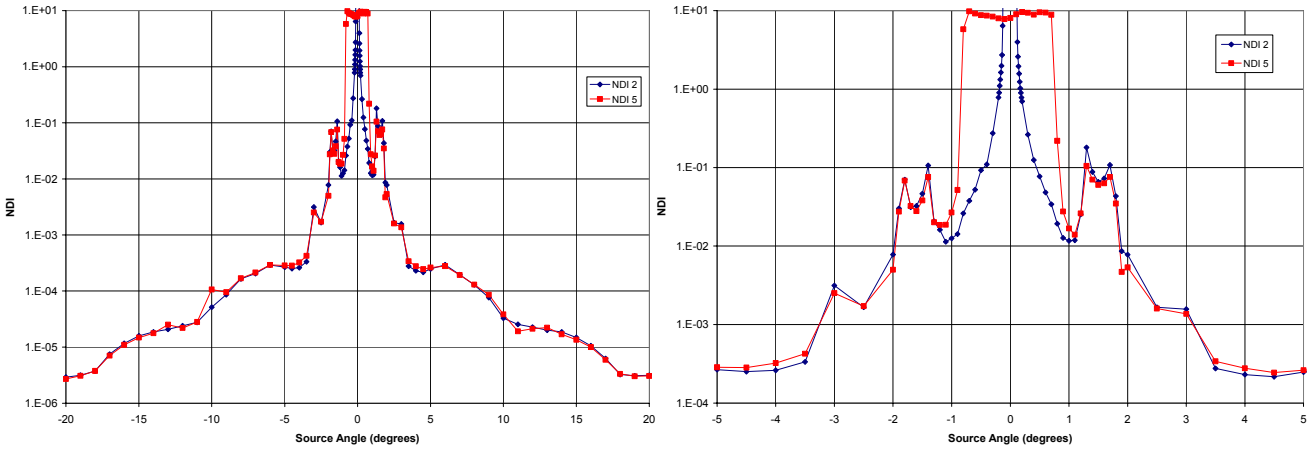

Figure 12. NDI comparison of ONC with small-field and full-field apertures.

4.2 Measurements 6 through 12

The flight ONC was returned to SDL on February 16, 2004 for retesting. The new measurements were made in place of the originally planned tests of the engineering model. An improved mounting fixture was delivered, which made vertical alignment of the sensor easier. The ONC was in the non-rotated position (Az = 0°) for Measurements 6, 7, and 8. Measurements 6 and 7 were center aperture tests, and Measurement 8 had the edge aperture in place. The results of the first test (No. 6) were good and bad. The humps at ±1.5° were not present, but the overall performance was worse than before. Once again a misalignment was found. Upon its delivery to SDL, the ONC was taken out of a cold vehicle into the warmer test facility where it was mounted and aligned. Apparently the ONC had not yet acclimated to the new environment. The next morning the unit was re-aligned and data taken. Measurements 6 and 7 are shown in comparison to the original ONC response (Measurement 2) in Figure 13. Figure 14 shows the small angle data of Measurements 2 and 7. The JPL modifications definitely improved performance. In addition to removal of the humps, the overall off-axis response is lower, which may indicate less contamination on the optics. The 1.2 mm aperture was placed at the left edge of the image plane for Measurement 8. Figure 15 shows a comparison of the small angle data to the "pre-fix" ONC response (i.e. Measurement 4). The better performance of the modified unit is apparent; however, both responses show a spike at –1.2°. Note that the later measurement has more character due to extra data points.

The ONC was rotated 90° (Az = 90°) for Measurements 9, 10, and 11. Measurement 9 (center aperture) had a slight misalignment. After a small vertical adjustment, Measurement 10 (repeat test) was made. Measurement 11 was a full-field test whose results will be shown in a later comparison. The ONC was rotated 45° (Az = 45°) for the final test (Measurement 12: center aperture). A comparison of Measurements 7, 10, and 12 at small angles is shown in Figure 16.

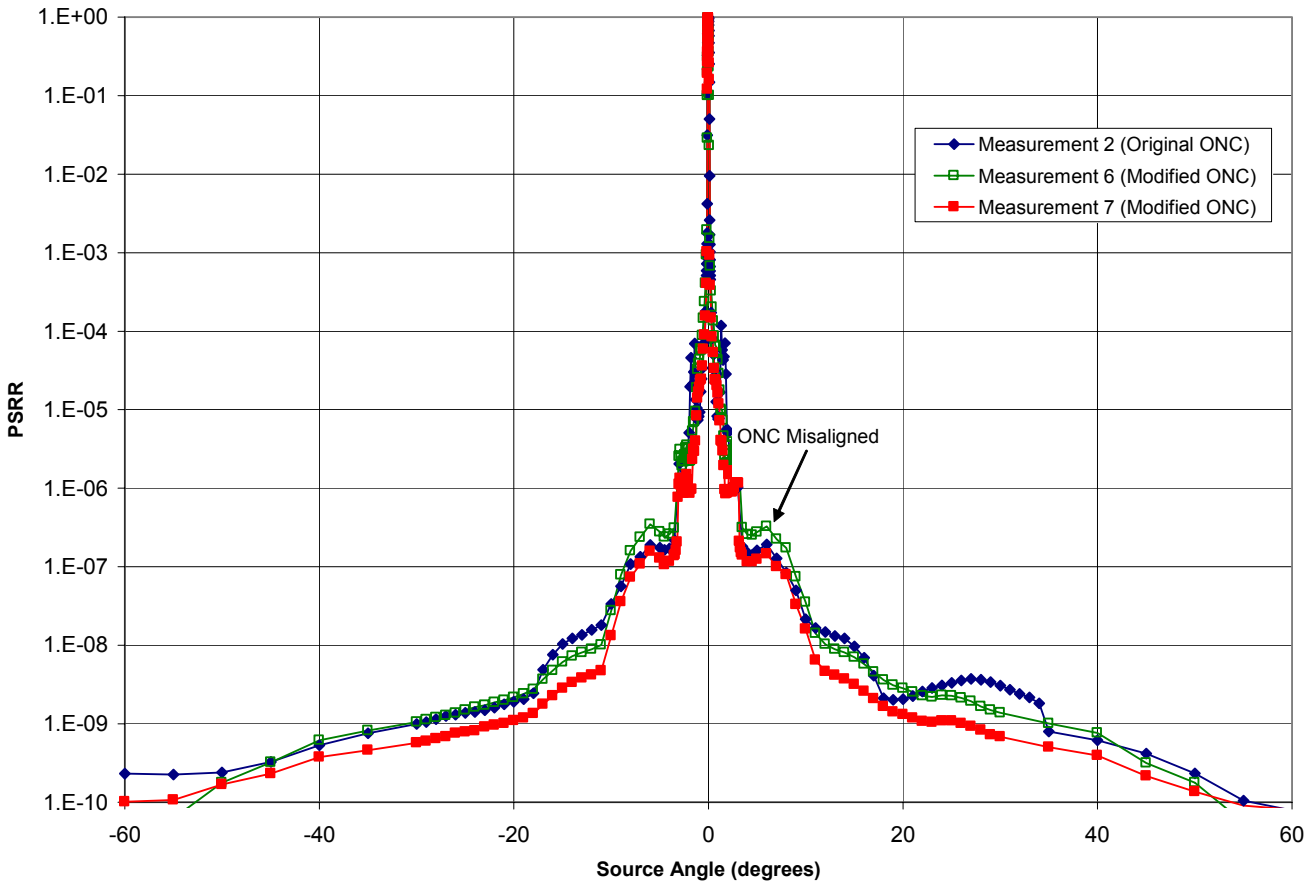

Figure 13. Measurements 2, 6, and 7 (center aperture): Original and modified flight unit.

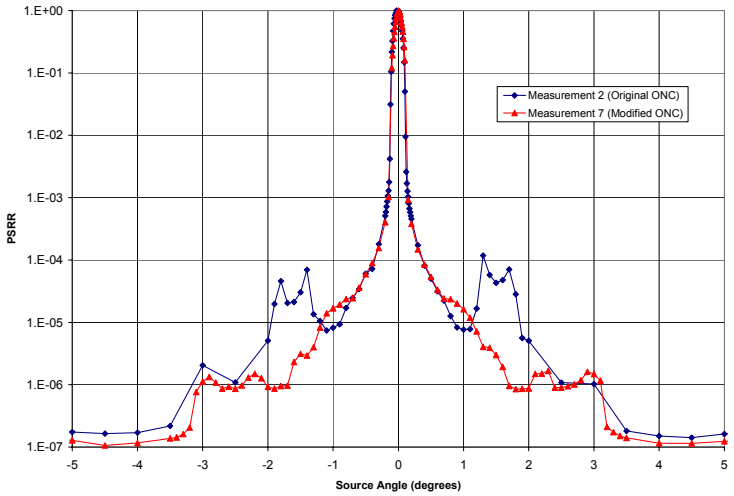

Figure 14. Measurements 2 and 7 (center aperture): Original and modified flight unit.

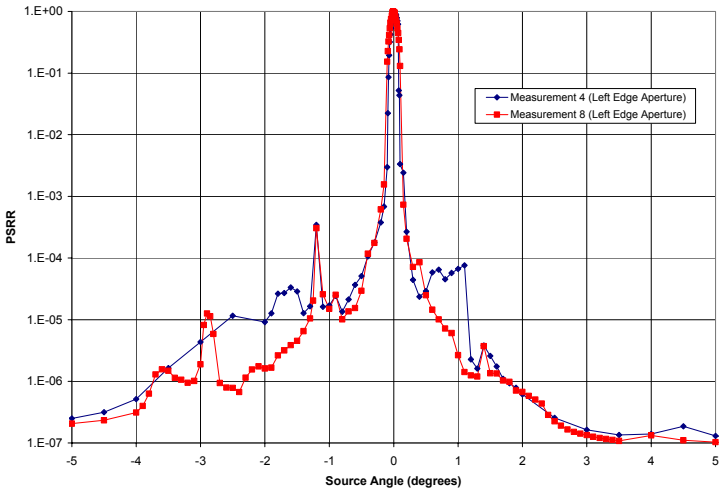

Figure 15. Measurements 4 and 8 (left edge aperture): Original and modified flight unit.

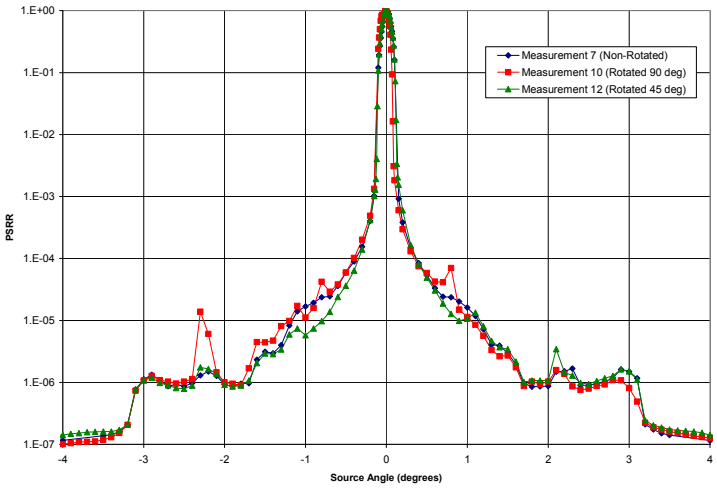

Figure 16. Measurements 7, 10, and 12 (center aperture): ONC rotations of 0°, 45°, and 90°.

5. COMPARISON OF THE RESULTS TO ASAP MODEL AND OTHER JPL CAMERAS

A stray light analysis of the ONC was performed by Breault Research Organization (BRO) using the Advanced Systems Analysis Program (ASAP[8]) software to estimate the off-axis response in NDI form. The accuracy of the model not only relies on the analyst including the significant stray light paths, but on the scatter model of the optical and mechanical surfaces. Uncertainties in both surface roughness and particulate contamination exist.

The ASAP generated NDI for a system transmission of 1.0 is compared to Measurements 7 and 11 in Figures 17. The BRO results and Measurement 11 use the entire image plane (i.e. full-field). Measurement 7 is the narrow-field response using the 1.2 mm center aperture. The measured response is higher than the predicted NDI at all source angles. A contributing factor in this is that the peak response of the PMT is near the short end of the ONC spectral band (0.45 μm), whereas the BRO analysis was made near the high end (0.65 μm). From the BRO report, it appears that the scatter function (i.e. BSDF) of the assumed 10 Å rms optical surfaces is defined near 0.6 μm. Since the measured off-axis response is due mainly to scatter from smooth surfaces, the results can be wavelength scaled (within reason) using

$$NDI_{\lambda 2} = \left(\frac{\lambda 1}{\lambda 2} \right)^{4+S} \times NDI_{\lambda 1} \tag{3}$$

where S is the slope of the scatter function plotted on a log-log scale. Using the BRO slope value of -1.9, the measured results can justifiably be scaled by *as much* as 0.55 for the comparison. The Measurement 11 NDI was scaled by this value and is included in Figure 17. The scaled results are in reasonable agreement with the software model for the angular ranges of 1° to 1.7° and 3.5° to 16°. From 1.7° to 3.5° the measurement picked up some significant stray light paths not present in the software model. At larger angles, one would expect a drop off in the response as the baffle shields the primary mirror from the source. Unlike the software prediction, the measured data does not indicate a drop. One possible explanation is that the source rays are hitting the non-vaned baffle tube at a high angle of incidence, leading to near specular scatter towards the mirror. It is also possible that the noise floor of the test setup (~1E-7 for the NDI) is being approached.

A final comparison is made between measurements of the ONC and two successful JPL planetary sensors. Figure 18 shows a stray light performance comparison of the ONC with the Galileo SSI and Cassini NAC sensors. Like the ONC, both are Cassegrain type systems with a refractive field corrector. The results of each of the cameras have been normalized to their respective solid angle FOVs to account for different focal lengths and detector sizes.

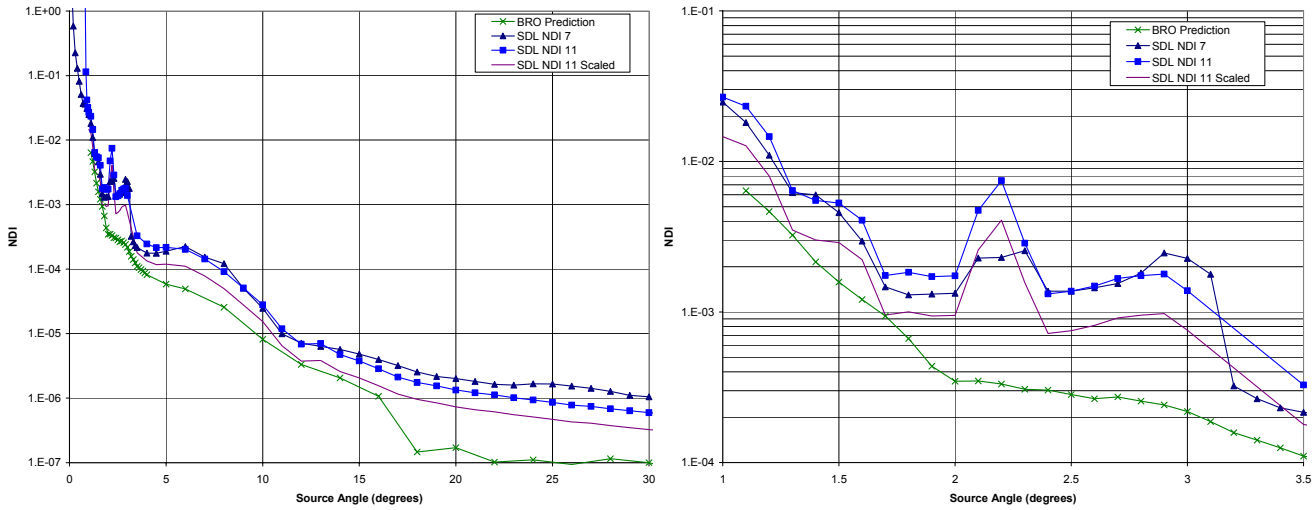

Figure 17. Comparison of predicted and measured off-axis responses.

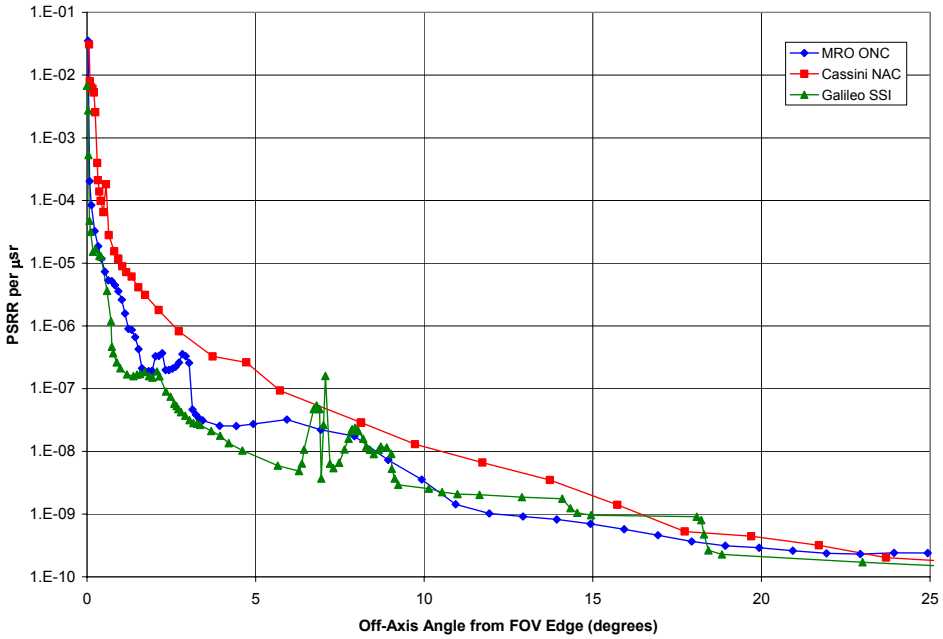

Figure 18. Off-axis response of JPL cameras (per µsr detector solid angle FOV).

6. CONCLUSIONS

The stray light performance of the Optical Navigation Camera of the Mars Reconnaissance Orbiter was measured at the Space Dynamics Laboratory of Utah State University in November 2003 and February 2004. The measurement was successful in two ways. First, it provided a crosscheck with the predicted software off-axis response. Second, and more important, a significant stray light path was identified and corrected. Several of the measurements had to be repeated due to a misalignment of the ONC with the collimated source. For the narrow-field tests, even a slight misalignment caused a "missing of the peak", leading to a false degradation in performance.

7. ACKNOWLEDGEMENTS

Research described in this paper was carried out at the Space Dynamics Laboratory, Utah State Univ., and Jet Propulsion Laboratory, California Institute of Technology, under contract with the National Aeronautics and Space Administration.

REFERENCES

1. MRO website: http:/mars4.jpl.nasa.gov/mro/
2. D. Milsom and G. Peterson, "Stray Light Design and Analysis of JPL's Optical Navigation Camera", BRO Report No. 4800, 2001.
3. C. Wyatt, "JPL Camera Optics Model SSI Optics No. 01 Calibration Report", No. 692534, Utah State University/Electro-Dynamics Laboratory, 1978.
4. J. Kemp, J. Stauder, S. Turcotte, "Terrestrial "Back Hole" for Measuring High-Rejection Off-Axis Response", Infrared Spaceborne Remote Sensing V, Proc. SPIE Vol. 3122, pp. 45-56, 1997.
5. J. Stauder et. al., "Off-Axis Response Measurement of the Sounding of the Atmosphere using Broadband Emission Radiometry (SABER) Telescope", Current Developments in Lens Design and Optical Engineering III, Proc. SPIE Vol. 4767, pp. 70-78, 2002.
6. Stray Light Measurement of the Mars Reconnaissance Orbiter Optical Navigation Camera, SDL/04-132, 2004.
7. Andrew E. Lowman, and John L. Stauder, "Stray light lessons learned from the Mars Reconnaissance Orbiter's Optical Navigation Camera," Stray Light in Optical Systems: Analysis, Measurement, and Suppression, Proc. SPIE, Vol. 5526B, pp. 240-248, 2004.
8. "ASAP stray light analysis software package, Version 7.0", Breault Research Organization 6400 East Grant Road, Suite 350, Tucson Arizona, 85715.